*Journal of Photochemistry*, *25* (1984) 131 - 143 

# RELAXATION OF THE $^1\Delta_g$ STATE IN PURE LIQUID OXYGEN AND IN LIQUID MIXTURES OF $^{16}O_2$ AND $^{18}O_2$†

E. WILD, H. KLINGSHIRN and MAX MAIER

*Naturwissenschaftliche Fakultät II — Physik, Universität Regensburg, 8400 Regensburg (F.R.G.)*

(Received January 4, 1984)

## Summary

We calculated the transition probability for collisional deactivation of the $^1\Delta_g$ state of $O_2$. The intersystem crossing transitions to the $v = 2$ and $v = 3$ vibrational levels of the electronic ground state are found to be dominant. The calculated ratio of the relaxation rate constants of the isotopes $^{18}O_2$ and $^{16}O_2$ is compared with the measured value ($50\ s^{-1}/2.3 \times 10^4\ s^{-1}$) in the liquid phase at $T = 77$ K. The measured $^1\Delta_g$ relaxation rate constants in liquid $^{16}O_2$–$^{18}O_2$ mixtures depend non-linearly on concentration. An explanation of the non-linear behaviour in terms of changes in the transition probability and the collision frequency in the mixtures is discussed.

## 1. Introduction

There has been recent progress [1, 2] in identifying successive steps of the relaxation routes of the $^1\Delta_g$ state in liquid $O_2$. First, there is an intersystem crossing to higher vibrational levels of the electronic ground state of $O_2$. It is followed by rapid vibrational–vibrational (V–V) energy transfer, populating the first vibrational level ($v = 1$) of the electronic ground state $^3\Sigma_g^-$. This level is deactivated slowly (milliseconds) by vibrational–translational (V–T) relaxation [1, 3]. At high $^1\Delta_g$ populations additional relaxation channels become important. It has been verified experimentally that the energy pooling reaction $^1\Delta_g + {}^1\Delta_g \rightarrow {}^1\Sigma_g^+ + {}^3\Sigma_g^-$ is one of these channels, which lead to a non-exponential decay of the $^1\Delta_g$ state [4].

Electronic-to-vibrational energy transfer has been shown to be responsible for quenching of the $^1\Delta_g$ state of $O_2$ in mixtures with diatomic molecules in the gas phase [5, 6]. This mechanism has also been suggested to cause quenching of $O_2(^1\Delta_g)$ in liquid solvents. It represents the basis of calculations [7, 8] and qualitative estimates [9] of the $^1\Delta_g$ quenching rate con-

†Paper presented at the COSMO 84 Conference on Singlet Molecular Oxygen, Clearwater Beach, FL, U.S.A., January 4 - 7, 1984.

0047-2670/84/$3.00 

stants. Recent experimental investigations [9 - 11] showed that the theory of Merkel and Kearns [7] reproduces correctly the qualitative trend but cannot provide quantitative values for the relaxation rate constants.

In this paper we present calculations of the relaxation rate constants for the collisional deactivation of the $^1\Delta_g$ state of $O_2$. They are compared with the results of experimental investigations of the $^1\Delta_g$ relaxation in liquid $^{16}O_2$, $^{18}O_2$ and liquid mixtures of these molecules at a temperature of 77 K. Using the theory of Schwartz, Slawsky and Herzfeld (SSH) [12 - 14] modified by Shin [15] to include the effect of attractive molecular forces we show that in pure $^{16}O_2$ and $^{18}O_2$ the electronic energy of the $^1\Delta_g$ state is primarily transferred to vibrational levels of the electronic ground state with quantum numbers $v = 2$ and $v = 3$. The measured and calculated ratios of the relaxation rate constants of liquid $^{16}O_2$ and $^{18}O_2$ are compared. The calculations are also applied to liquid $^{16}O_2$–$^{18}O_2$ mixtures to explain the observed non-linear dependence of the $^1\Delta_g$ relaxation rate constant on the $^{16}O_2$ concentration. The influence of the concentration dependence of the collision frequency on the relaxation rate constants in the liquid mixtures is discussed.

## 2. Pure liquids

### *2.1. Experimental details*

The apparatus is shown in Fig. 1. The $^1\Delta_g$ state of the $O_2$ molecules is excited by absorption of the light pulse of a $Q$-switched Nd:YAG laser with a pulse duration of about 20 ns and an energy of up to 20 mJ. The laser power is monitored by photodiode PD. The energy density distribution over the cross section of the laser beam is measured by the photodiode array PDA. The Nd:YAG laser light is focused with lens L (focal length $f = 100$ cm) into the cryostat containing liquid $O_2$. The population of the $^1\Delta_g$ state is monitored by observing fluorescence light at 635 nm due to the double-molecule transition $2\,^1\Delta_g \rightarrow 2\,^3\Sigma_g^- + h\nu$ with photomultiplier PM. The photomultiplier signal is fed to a photon counting system and a computer. The signals are averaged over about 1000 laser pulses. Stray light discrimination and spectral selection are obtained by narrow bandwidth interference filters

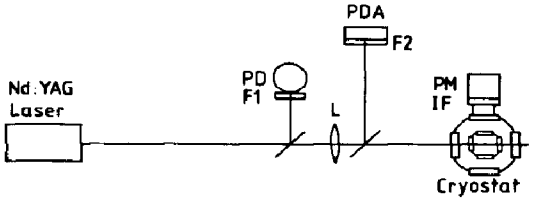


Fig. 1. Schematic diagram of the apparatus for measuring the time dependence of the double-molecule fluorescence at 635 nm from the $^1\Delta_g$ state in liquid $O_2$: PD, photodiode; PDA, photodiode array; PM, photomultiplier; L, lens; F1, F2, filters; IF, interference filter.

IF. The measurements were carried out at 77 K in a liquid nitrogen cryostat. High purity grade natural $O_2$ (Linde; purity, 99.999 vol.%; 0.2% $^{18}O$) and $^{18}O_2$ (Ventron) were used.

We measured the double-molecule fluorescence at 635 nm from the $^1\Delta_g$ state as a function of time for liquid natural $O_2$ and $^{18}O_2$. A relaxation rate constant of $k_1 = 2.3 \times 10^4\ s^{-1}$ was determined from the exponential decay of $O_2(^1\Delta_g)$. The decay constant of the $^1\Delta_g$ state in liquid $^{18}O_2$ depends on the number density $N^*$ of excited $^{18}O_2(^1\Delta_g)$ molecules. For number densities $N^* \gg 10^{16}\ cm^{-3}$ a non-exponential decay of the $^1\Delta_g$ state was observed [4]. By using the photon counting system we were able to measure at small $^1\Delta_g$ number densities $N^* < 10^{16}\ cm^{-3}$. Figure 2 shows an example of a measurement at low $^1\Delta_g$ population. The logarithm of the normalized fluorescence power $P_F/P_0$ at 635 nm (curve 1) is plotted against time $t$ for a number density $N^* = 8 \times 10^{15}\ cm^{-3}$ of $^{18}O_2(^1\Delta_g)$ molecules. The measured curve follows a straight line, *i.e.* there is an exponential decay (for $N^* < 10^{16}\ cm^{-3}$). From the slope of the curve we determine a relaxation rate constant $k_2$ of the $^1\Delta_g$ state of $50 \pm 5\ s^{-1}$ for liquid $^{18}O_2$ at $T = 77$ K. Within the experimental accuracy we obtained the same result for $O_2$ samples containing 99.8% and 99.0% $^{18}O_2$. In ref. 4 the relaxation rate constant of $^{18}O_2$ was determined from *non*-exponential decay curves. By fitting calculated curves to the experimental curves a value of $k_2 = 100 \pm 50\ s^{-1}$ was obtained. Both the new and the old values agree within the experimental accuracy.

It has been shown that the energy pooling reaction $^1\Delta_g + {}^1\Delta_g \rightarrow {}^1\Sigma_g^+ + {}^3\Sigma_g^-$ populates the second excited $^1\Sigma_g^+$ state of $^{18}O_2$ [4]. We observed fluorescence light at 765 nm from the $^1\Sigma_g^+$ state. In Fig. 2 the logarithm of the fluorescence power at 765 nm is plotted *versus* time $t$ (curve 2). The single-molecule fluorescence at 765 nm (curve 2) decays with the same time constant as the double-molecule fluorescence at 635 nm (curve 1). This

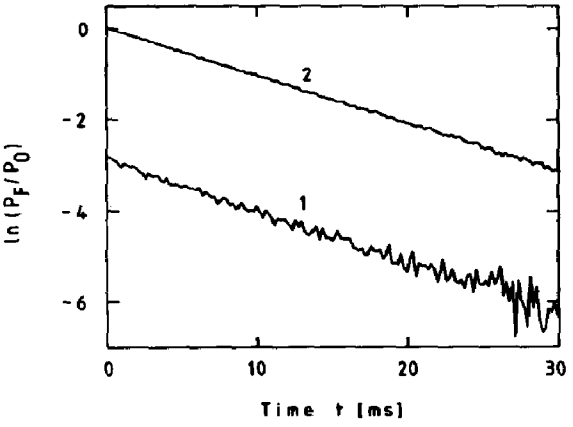


Fig. 2. Logarithm of the normalized fluorescence power $P_F/P_0$ *vs.* time $t$ for liquid $^{18}O_2$ at 77 K ($P_0$ is the fluorescence power of curve 2 at $t = 0$): curve 1, double-molecule fluorescence at 635 nm from the $^1\Delta_g$ state (number density $N^* = 8 \times 10^{15}\ cm^{-3}$ of $^{18}O_2(^1\Delta_g)$); curve 2, single-molecule fluorescence at 765 nm from the $^1\Sigma_g^+$ state ($N^* = 2 \times 10^{15}\ cm^{-3}$).

result can be understood from the fact that both the energy pooling reaction and the double-molecule fluorescence signal are proportional to the square of the $^1\Delta_g$ population. It should be noted that the $^1\Sigma_g^+$ fluorescence (curve 2) and the $2\,^1\Delta_g$ fluorescence (curve 1) were measured in different runs, in which the concentration of excited $^{18}O_2(^1\Delta_g)$ was smaller for curve 2 ($N^* = 2 \times 10^{15}$ cm$^{-3}$) than for curve 1 ($N^* = 8 \times 10^{15}$ cm$^{-3}$). In spite of the smaller $^{18}O_2(^1\Delta_g)$ concentration the $^1\Sigma_g^+$ fluorescence signal is much larger than the $2\,^1\Delta_g$ signal, indicating that the energy pooling reaction is a very efficient process in liquid $^{18}O_2$.

### *2.2. Model of $^1\Delta_g$ excitation and relaxation*

The excitation and relaxation of the $^1\Delta_g$ state in liquid $O_2$ have been discussed in ref. 1. We summarize briefly the main results which are necessary to understand the experimental results and the calculations of the transition probability.

The Nd:YAG laser pulse excites the $^1\Delta_g(v = 1)$ and $^1\Delta_g(v = 0)$ states. Since the $^1\Delta_g(v = 1)$ state relaxes rapidly to the $^1\Delta_g(v = 0)$ state, the final result of the absorption is the population of the $^1\Delta_g(v = 0)$ state.

Relaxation of the $^1\Delta_g$ state by emission of radiation can be neglected since the radiative rate constants are known to be small in $O_2$. The collisional deactivation proceeds in several steps.

(i) The first step, electronic–vibrational intersystem crossing, determines the relaxation rate constant $k$ of the $^1\Delta_g$ state. The electronic energy of the $^1\Delta_g$ state is transferred to higher vibrational levels of the $^3\Sigma_g^-$ electronic ground state (Fig. 3):

$$^1\Delta_g(v' = 0) + {}^3\Sigma_g^-(v' = 0) \xrightarrow{k} {}^3\Sigma_g^-(v) + {}^3\Sigma_g^-(5 - v) + \Delta E_v \qquad (1)$$

The energy mismatch $\Delta E_v$ is given by

$$\Delta E_v = E_\Delta - (E_v + E_{5-v}) \qquad (2)$$

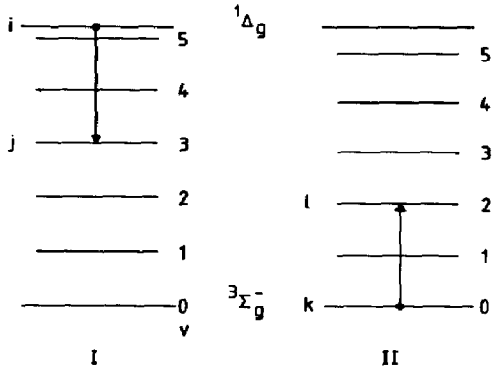


Fig. 3. Transitions between energy levels of molecules I and II. The energy levels correspond to the special case of $^{16}O_2$ (molecule I) and $^{18}O_2$ (molecule II).

where $E_\Delta$ and $E_v$ are the energies of the $^1\Delta_g$ state and the $^3\Sigma_g^-(v)$ state respectively. The energy $\Delta E_v$ is transferred to translational motion. Different relaxation routes are distinguished by the vibrational quantum numbers $v$ = 0 - 5. Our calculations in the next section show that the relaxation routes involving the vibrational levels with $v = 2$ and $v = 3$ are dominant. It should be mentioned that the transfer of the electronic energy of the $^1\Delta_g$ state to vibrational levels of the electronic ground state has also been observed experimentally in mixtures of $O_2$ with various diatomic molecules in the gas phase [5, 6].

(ii) In the second step, relaxation of the vibrational levels of the electronic ground state of $O_2$, the vibrationally excited states $^3\Sigma_g^-(v > 1)$ decay to the $^3\Sigma_g^-(v = 1)$ state primarily by near-resonant V–V transfer, which is a very rapid process. The last step of the relaxation is the collisional deactivation of the $^3\Sigma_g^-(v = 1)$ state by slow V–T transfer ($\tau$ = 2.5 ms in natural liquid $O_2$ at $T$ = 77 K [1]). These relaxation steps have been confirmed experimentally in liquid natural $O_2$ by observing the $^3\Sigma_g^-(v = 1)$ population as a function of time [1].

*2.3. Calculations of the transition probability*

Merkel and Kearns developed a theory of quenching of $O_2(^1\Delta_g)$ by solvent molecules in terms of intermolecular electronic-to-vibrational energy transfer [7, 8]. The $^1\Delta_g$ relaxation rate constant was related to the intensities of IR overtone and combinational absorption bands of the solvent in the wavelength regions of $^1\Delta_g \rightarrow {}^3\Sigma_g^-$ transitions, especially near 1.27 and 1.59 $\mu$m. Recent experimental investigations [9 - 11] show that a quantitative correlation between calculated and measured quenching rate constants is lacking, although a qualitative trend is evident. For pure $O_2$ the model of Merkel and Kearns cannot explain the observed large difference between the $^1\Delta_g$ relaxation rate constants of $^{16}O_2$ and $^{18}O_2$, because the IR absorption at 1.27 $\mu$m is about the same for both isotopes and absorption at 1.59 $\mu$m is negligible. Hurst and Schuster [9] suggested a semiquantitative model of the $O_2(^1\Delta_g)$ relaxation in solution which is based on the repulsive interaction between $O_2$ and solvent molecules. The relaxation rate constant given in their paper contains the same basic factors as obtained below from the SSH theory [12 - 15].

Theoretical approaches to calculate the transition probability for the collisional deactivation of the second excited electronic $^1\Sigma_g^+$ state of $O_2$ took into account short-range [16, 17] and long-range [18, 19] intermolecular forces. Kear and Abrahamson [16] developed a theory of quenching of $O_2(^1\Sigma_g^+)$ which is based on the SSH theory of vibrational relaxation [12] and an extension to electronic relaxation by Dickens *et al.* [17]. Although the theories are successful in explaining the quenching of $O_2(^1\Sigma_g^+)$ by other diatomic molecules, they fail to reproduce the experimental results on pure $O_2$.

In this paper we use the SSH theory [12 - 14], modified by Shin [15] to include attractive forces, to calculate the transition probabilities for the

collisional deactivation of the $^1\Delta_g$ state. Although there are several defects of the theory which limit the accuracy of the calculations, it accounts for the principal features of energy transfer and illustrates the relative importance of the various factors which influence the transfer probabilities.

The theory was developed for transitions between vibrational levels of the same electronic state. We apply it to transitions where the electronic state changes. The corresponding changes in the transition probability are taken into account by multiplying the results by a constant factor $P_\Delta$ [17]. In the first approximation we assume that the equilibrium distances of the oxygen nuclei and the curvatures of the potential curves of the $^3\Sigma_g^-$ and $^1\Delta_g$ states of $O_2$ are the same [20]. The attractive forces between the molecules are taken into account by using the Morse potential [15]:

$$V(r) = \epsilon \exp\{-\alpha(r - r_m)\} - 2\epsilon \exp\left\{-\frac{1}{2}\alpha(r - r_m)\right\} \tag{3}$$

Here $\epsilon$ is the depth of the potential and $\alpha$ is a measure of the range of the intermolecular forces. The probability $P_{k,l}^{i,j}$ that during a binary collision molecule I will change its quantum state from $i$ to $j$, while simultaneously molecule II will change its state from $k$ to $l$ (see Fig. 3), is given by [13]

$$P_{k,l}^{i,j} = \bar{P}\{V^{i,j}(\mathrm{I})\}^2\{V^{k,l}(\mathrm{II})\}^2 f(\Delta E_v) \tag{4}$$

The factor $\bar{P}$ contains various terms, *e.g.* steric factors, $P_\Delta$ etc. The vibrational factor $\{V^{i,j}(\mathrm{I})\}^2$ is the square of the matrix element for the transition between vibrational states $i$ and $j$ of molecule I. As discussed in the preceding section the decay routes of the $^1\Delta_g$ state include transitions between states $i = 0$ and $j = v$ of molecule I and $k = 0$ and $l = 5 - v$ of molecule II (see eqn. (1) and Fig. 3). In the first approximation we use the wavefunctions of a harmonic oscillator and obtain for homonuclear diatomic molecules

$$\{V^{0,v}(\mathrm{I})\}^2\{V^{0,5-v}(\mathrm{II})\}^2 = \left(\frac{h\alpha^2}{8\pi^2}\right)^5 \left(\frac{\overline{A_\mathrm{I}^2}}{\nu_{0\mathrm{I}}}\right)^v \left(\frac{\overline{A_\mathrm{II}^2}}{\nu_{0\mathrm{II}}}\right)^{5-v} \frac{1}{v!(5-v)!} \tag{5}$$

$\nu_{0\mathrm{I}}$ and $\nu_{0\mathrm{II}}$ are the vibrational frequencies of molecules I and II respectively. $\overline{A_\mathrm{I}^2}$ and $\overline{A_\mathrm{II}^2}$ are the average vibrational amplitude coefficients which are given in ref. 21. (Owing to a misprint in ref. 21, p. 46, a factor 1/2 is missing in the vibrational amplitude coefficients $\overline{A^2}$.) It is interesting to note that the different relaxation channels enter eqn. (5) only via the vibrational quantum number $v$. The dependence of the transition probability on the energy mismatch $\Delta E_v$ is contained in the factor $f$ of eqn. (4) which is written as

$$f(\Delta E_v) = \left(\frac{8\pi^3\mu\,\Delta E_v}{\alpha^2 h^2}\right)^2 \zeta^{1/2} \exp\left\{-3\zeta + \frac{4}{\pi}\left(\frac{\epsilon\zeta}{k_\mathrm{B}T}\right)^{1/2} + \frac{\Delta E_v}{2k_\mathrm{B}T} + \frac{16\epsilon}{3\pi^2 k_\mathrm{B}T}\right\} \tag{6}$$

The abbreviation $\zeta$ is given by

$$\zeta = \left( \frac{2\pi^4 \mu \, \Delta E_v^2}{\alpha^2 h^2 k_B T} \right)^{1/3} \tag{7}$$

where $\mu$ is the reduced mass of the colliding pair.

For the calculation of the transition probability we need values of the potential parameters $\alpha$ and $\epsilon$ of oxygen. We use a value of $\epsilon/k_B = 109$ K, which is the mean value of the numerals given in ref. 22. The parameter $\alpha$ depends slightly on temperature. It is given in ref. 21 for a purely repulsive potential for various temperatures ($T > 300$ K). For a temperature of 77 K no value is available. We determined $\alpha$ by fitting the calculated ratio of the transition probabilities of $^{18}O_2$ and $^{16}O_2$ to the experimental result.

The transition probability $P_{0,5-v}^{0,v}$ is calculated from eqns. (4) - (7) for pure $^{16}O_2$ and for pure $^{18}O_2$. The results are normalized to the sum of the probabilities

$$\sum_{v=0}^{5} P_{0,5-v}^{0,v} = P_1$$

of $^{16}O_2$. The calculated ratio $P_2/P_1$ of the transition probabilities of $^{18}O_2$ and $^{16}O_2$ is compared with the measured ratio $k_2/k_1$ of the relaxation rate constants. In the comparison we assumed that the collision frequencies are the same in liquid $^{18}O_2$ and $^{16}O_2$. The best agreement with the measured ratio of $k_2/k_1 = 50 \text{ s}^{-1}/2.3 \times 10^4 \text{ s}^{-1} = 2.2 \times 10^{-3}$ (see Section 2.1) is obtained for a value of $\alpha = 5.53 \times 10^8 \text{ cm}^{-1}$. This number is larger than $\alpha = 5.377 \times 10^8 \text{ cm}^{-1}$ at room temperature given by Lambert [21]. The difference is believed to be mainly due to the different temperatures, because $\alpha$ is known to increase with decreasing temperature [21].

The results of our calculations are summarized in Table 1. It is interesting to note that in $^{16}O_2$ and $^{18}O_2$ the probability is largest for transitions from the $^1\Delta_g$ state to the $^3\Sigma_g^-(v = 2)$ and $^3\Sigma_g^-(v = 3)$ states. This result is expected from qualitative considerations because the energy mismatch $\Delta E_v$ (see Table 1) is smallest and the vibrational factor (see eqn. (5)) is largest for these transitions. The transition probability $P_2$ of $^{18}O_2$ is much smaller than that of $^{16}O_2$ because of the larger energy $\Delta E_v$ of $^{18}O_2$ (see Table 1) which has to be transferred to translational energy.

## 3. Liquid $^{16}O_2$–$^{18}O_2$ mixtures

### *3.1. Experimental results*

The experiments in liquid $^{16}O_2$–$^{18}O_2$ mixtures were carried out in the same way as for the pure liquids (see Section 2.1). We measured the double-molecule fluorescence power at 635 nm from the $^1\Delta_g$ state for various concentrations $x$ of $^{16}O_2$. It should be noted that we did not distinguish between the fluorescence from $^{16}O_2$ and $^{18}O_2$ molecules, which have about the same electronic energy of the $^1\Delta_g$ state [4]. We measured the sum of the fluores-

TABLE 1

Normalized probability $P^{0,v}_{0,5-v}/P_1$ for transitions between vibrational states 0 and $v$ of molecule I and vibrational states 0 and $5-v$ of molecule II

| *Vibrational state v of I* | *Vibrational state 5 — v of II* | $\Delta E_v$[a] ($cm^{-1}$) | $(P^{0,v}_{0,5-v}/P_1)\times 10^2$ | $\sum_{v=0}^{5} P^{0,v}_{0,5-v}/P_1$ |
|---|---|---|---|---|
| $^{16}O_2$ | $^{16}O_2$ | | | 1.00 |
| 0 | 5 | 313 | 0.7 | |
| 1 | 4 | 221 | 10.7 | |
| 2 | 3 | 174 | 38.6 | |
| 3 | 2 | 174 | 38.6 | |
| 4 | 1 | 221 | 10.7 | |
| 5 | 0 | 313 | 0.7 | |
| $^{18}O_2$ | $^{18}O_2$ | | | $2.2\times10^{-3}$ |
| 0 | 5 | 726 | 0.002 | |
| 1 | 4 | 644 | 0.025 | |
| 2 | 3 | 603 | 0.082 | |
| 3 | 2 | 603 | 0.082 | |
| 4 | 1 | 644 | 0.025 | |
| 5 | 0 | 726 | 0.002 | |
| $^{16}O_2$ | $^{18}O_2$ | | | $7.9\times10^{-2}$ |
| 0 | 5 | 726 | 0.003 | |
| 1 | 4 | 556 | 0.105 | |
| 2 | 3 | 429 | 1.057 | |
| 3 | 2 | 347 | 3.237 | |
| 4 | 1 | 308 | 2.882 | |
| 5 | 0 | 313 | 0.573 | |

Calculated for values of the potential parameters of $\epsilon/k_B = 109$ K and $\alpha = 5.53\times10^8$ $cm^{-1}$. $\Delta E_v$ is the energy mismatch in the collision according to eqns. (1) and (2).
[a] From ref. 4.

cence signals of both components of the mixture. The relaxation rate constants were determined from the time decay of the fluorescence curves.

In Fig. 4 the measured relaxation rate constants $k(x)$ normalized to the rate constant $k(1) \equiv k_1$ of pure liquid $^{16}O_2$ are plotted against the $^{16}O_2$ concentration $x$. The open circles represent the experimental points. The full and broken lines are calculated curves (see Sections 3.2.2 and 3.2.3). It is important to note that there is a non-linear concentration dependence of the relaxation rate constant, which will be discussed in detail in the following sections.

### *3.2. Discussion*

#### *3.2.1. Differential equations*

The time dependence of the population of the $^1\Delta_g$ state of $O_2$ is governed by the deactivation by collisions with $^{16}O_2$ and $^{18}O_2$ molecules and

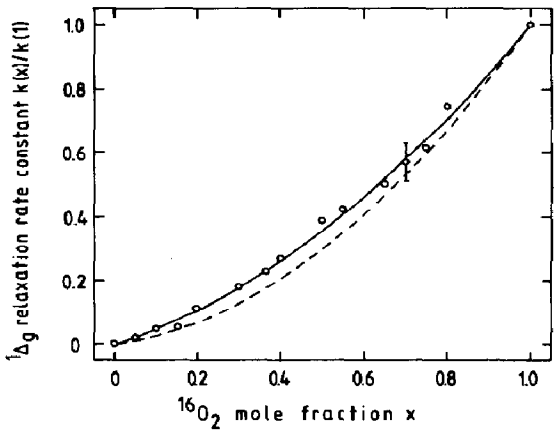


Fig. 4. Relaxation rate constant $k(x)/k(1)$ of the $^1\Delta_g$ state in liquid $^{16}O_2$–$^{18}O_2$ mixtures *vs.* the $^{16}O_2$ concentration $x$: ○, experimental points; ——, — — —, calculated curves.

the migration of the electronic energy in the liquid mixture. The differential equations for the number densities $N^*$ of $O_2(^1\Delta_g)$ are written as

$$\frac{dN_1^*}{dt} = -\{\bar{k}_{11}(x) + \bar{k}_{12}(x)\}N_1^* - \bar{k}_m(x)N_1^* + \bar{k}_m'(x)N_2^* \tag{8}$$

$$\frac{dN_2^*}{dt} = -\{\bar{k}_{21}(x) + \bar{k}_{22}(x)\}N_2^* + \bar{k}_m(x)N_1^* - \bar{k}_m'(x)N_2^* \tag{9}$$

The subscripts 1 and 2 stand for $^{16}O_2$ and $^{18}O_2$ respectively. The transfer of electronic energy from $^{16}O_2$ to $^{18}O_2$ and vice versa occurs with rate constants $\bar{k}_m$ and $\bar{k}_m'$ respectively. Since the electronic energies of the $^1\Delta_g$ states of $^{16}O_2$ and $^{18}O_2$ are about the same [4], we assume that $\bar{k}_m \approx \bar{k}_m'$. Gas phase measurements [23] have shown that the electronic energy transfer occurs at least once in every ten collisions, *i.e.* it is a very rapid process compared with the deactivation.

The first terms on the right-hand sides of eqns. (8) and (9) represent the collisional deactivation of the excited molecules. The rate constant $\bar{k}_{ij}$ describes the deactivation of excited molecule $i$ by ground state molecule $j$. According to the isolated binary collision model [24] it may be expressed by the collision frequency $Z_{ij}$ and the transition probability $P_{ij}$ as

$$\bar{k}_{ij} = P_{ij}Z_{ij} \tag{10}$$

In contrast with gases the calculation of $Z_{ij}$ is not a simple problem in liquids. There are several ways of calculating the collision frequency in the liquid phase [25 - 31]. We use here the relation given by Einwohner and Alder [31]:

$$Z_{ij} = 4R^2\left(\frac{\pi k_B T}{m}\right)^{1/2} g_{ij}(R)N_j \tag{11}$$

$g_{ij}(R)$ is the pair distribution function at the molecular distance $R$ where the deactivation is assumed to occur. When the molecules are represented by hard spheres with diameter $\sigma$, the pair distribution function has to be taken at $R = \sigma$. $m$ is the molecular mass and $N_j$ the number density of ground state $O_2$ molecules responsible for the deactivation of $O_2(^1\Delta_g)$. The number densities of $^{16}O_2$ and $^{18}O_2$ molecules are related to the $^{16}O_2$ concentration $x$ by $N_1 = Nx$ and $N_2 = N(1-x)$ respectively. $N$ is the total number density of molecules. In general, the pair distribution function $g_{ij}$ in a mixture depends on concentration, leading to a non-linear concentration dependence of $Z_{ij}$ and $\bar{k}_{ij}$.

For a calculation of the pair distribution functions we approximate the molecules by hard spheres with diameter $\sigma$. The pair distribution functions at contact distance $\sigma$ are given in refs. 32 and 33. In the special case of isotope mixtures the hard sphere diameters $\sigma$ of the excited and ground state molecules of both components are equal in a good approximation. The pair distribution functions $g_{ij}(\sigma) = g$ are then independent of concentration $x$ and the same for all combinations of $i$ and $j$ [32, 33]. In this case, the collision frequencies in the liquid mixtures depend linearly on the $^{16}O_2$ concentration $x$ because of the factor $N_j$ in eqn. (11). We introduce eqns. (10) and (11) into eqns. (8) and (9). Using the abbreviation

$$k_{ij} = 4\sigma^2\left(\frac{\pi k_B T}{m}\right)^{1/2} gNP_{ij} \tag{12}$$

we obtain

$$\frac{dN_1^*}{dt} = -\{k_1 x + k_{12}(1-x)\}N_1^* - k_m(1-x)N_1^* + k_m x N_2^* \tag{13}$$

$$\frac{dN_2^*}{dt} = -\{k_{21} x + k_2(1-x)\}N_2^* + k_m(1-x)N_1^* - k_m x N_2^* \tag{14}$$

Here $k_{11} \equiv k_1$ and $k_{22} \equiv k_2$ are the relaxation rate constants of pure $^{16}O_2$ and $^{18}O_2$ respectively.

*3.2.2. Solution of the differential equations*

Equations (13) and (14) have been solved exactly. For the discussion of the experimental results it is sufficient to give an approximate solution for $k_m \gg k_1, k_2$. This condition is fulfilled in our experiments since the energy migration is rapid compared with the deactivation processes. We assume that we have a rapid dynamical equilibrium between excited $^{16}O_2$ and $^{18}O_2$ molecules for times $t$ long compared with the energy migration time $1/k_m$. In this case we obtain

$$\begin{aligned} N_1^* &= xN^* \\ N_2^* &= (1-x)N^* \end{aligned} \tag{15}$$

*i.e.* the ratio of the number densities of the excited molecules is equal to that of the ground state molecules. $N^* = N_1^* + N_2^*$ is the total number density of the excited molecules. In the experiments we observed the total fluorescence signal from $^{16}O_2$ and $^{18}O_2$. We add therefore eqns. (13) and (14) and substitute eqn. (15) into the resulting equation to obtain a differential equation for $N^*$. The solution of this equation is given by

$$N^* = N_0^* \exp\{-k(x)t\} \tag{16}$$

$N_0^*$ is the initial total number density of the molecules after excitation by the pump laser pulse. The relaxation rate constant in the mixtures is given by

$$k(x) = x^2\{k_1 + k_2 - (k_{12} + k_{21})\} + x(k_{12} + k_{21} - 2k_2) + k_2 \tag{17}$$

It depends non-linearly on the $^{16}O_2$ concentration $x$. The rate constants $k_1$ and $k_2$ are known from investigations of the pure liquids (see Section 2.1). The quantity $k_{12} + k_{21}$ is determined by fitting the results of eqn. (17) to the measured points in Fig. 4. The best agreement between theory and experiments is obtained for $(k_{12} + k_{21})/k_1 = 0.43$ (the full line in Fig. 4). In the following section $k_{12} + k_{21}$ is calculated using the SSH theory and compared with the number obtained from the fit.

It is interesting to consider the special case where the sum of the relaxation rate constants in the pure liquids is equal to the sum of the mutual relaxation rate constants of both components in the mixture, *i.e.* $k_1 + k_2 = k_{12} + k_{21}$. In this case the quadratic term in eqn. (17) vanishes and we obtain a linear dependence of $k(x)$ on concentration. The observed non-linear dependence would then have to be attributed to a different physical mechanism.

*3.2.3. Calculations of the transition probabilities*

In liquid mixtures of $^{16}O_2$ and $^{18}O_2$ combinations of the different vibrational levels lead to additional relaxation channels which are not present in the pure liquids. The energy mismatches $\Delta E_v$ for these channels are given in Table 1. They range from $\Delta E_v = 308\ cm^{-1}$ to $\Delta E_v = 726\ cm^{-1}$. We calculated the transition probabilities for the deactivation of $^{16}O_2(^1\Delta_g)$ by $^{18}O_2$ using eqns. (4) - (7). The results in Table 1 show that the following relaxation channels with $v = 3$ (see Fig. 3) and $v = 4$ are dominant:

$$^{16}O_2\{^1\Delta_g(v' = 0)\} + {}^{18}O_2\{^3\Sigma_g^-(v' = 0)\} \longrightarrow {}^{16}O_2\{^3\Sigma_g^-(v)\} + {}^{18}O_2\{^3\Sigma_g^-(5 - v)\} \tag{18}$$

The relaxation routes with $v = 2$ and $v = 5$ are less important.

The relaxation rate constants of the $O_2$ isotopes are assumed to be proportional to the transition probabilities (see eqn. (12)). Using the values given in Table 1, fourth column, for $^{16}O_2$–$^{18}O_2$ we obtain

$$\frac{k_{12}}{k_1} = \frac{P_{12}}{P_1} = 7.9 \times 10^{-2}$$

The transition probability $P_{12} = \Sigma_{v=0}^{5} P_{0,5-v}^{0,v}$ for deactivation of $^{16}O_2$ by $^{18}O_2$ is equal to $P_{21}$ for deactivation of $^{18}O_2$ by $^{16}O_2$, *i.e.* $k_{21} = k_{12}$. We calculated the relaxation rate constant $k(x)$ from eqn. (17) for a value of $(k_{12} + k_{21})/k_1 = 0.158$. The result is shown as a broken line in Fig. 4. There is a difference between the calculated and fitted values of $k_{12}$, which may be due to the following points. (i) The calculations of the transition probabilities are not very accurate because of the limitations of the SSH theory. (ii) The assumption of a linear concentration dependence of the collision frequencies in liquid isotope mixtures may not be strictly correct.

Experiments on *gas* mixtures of $^{16}O_2$ and $^{18}O_2$ are in progress to clarify the origin of the observed difference between the calculated and the measured concentration dependence of the $^1\Delta_g$ relaxation rate constants. Gas mixtures will allow a more accurate comparison between the measured rate constants and the calculated transition probabilities because the calculation of the collision frequencies is straightforward in gases. In addition, the comparison between the results in the gas and in the liquid phase should provide information on the validity of various models for the calculation of collision frequencies in liquid mixtures.

## Acknowledgments

The authors gratefully acknowledge financial support by the Deutsche Forschungsgemeinschaft. They thank Dr. J. Chesnoy and Dr. M. Chatelet for valuable discussions.

## References

1 E. Wild, H. Klingshirn, B. Faltermeier and M. Maier, *Chem. Phys. Lett.*, *93* (1982) 490.
2 J. G. Parker, *J. Chem. Phys.*, *67* (1977) 5352, and references cited therein.
3 R. Protz and M. Maier, *Chem. Phys. Lett.*, *64* (1979) 27.
4 H. Klingshirn, B. Faltermeier, W. Hengl and M. Maier, *Chem. Phys. Lett.*, *93* (1982) 485.
5 S. Madronich, J. R. Wiesenfeld and G. J. Wolga, *Chem. Phys. Lett.*, *46* (1977) 267.
6 E. A. Ogryzlo and B. A. Thrush, *Chem. Phys. Lett.*, *23* (1973) 34.
7 P. B. Merkel and D. R. Kearns, *J. Am. Chem. Soc.*, *94* (1972) 7244.
8 C. A. Long and D. R. Kearns, *J. Am. Chem. Soc.*, *97* (1975) 2018.
9 J. R. Hurst and G. B. Schuster, *J. Am. Chem. Soc.*, *105* (1983) 5756.
10 P. R. Ogilby and C. S. Foote, *J. Am. Chem. Soc.*, *105* (1983) 3423.
11 M. A. J. Rodgers, *J. Am. Chem. Soc.*, *105* (1983) 6201.
12 R. N. Schwartz, Z. I. Slawsky and K. F. Herzfeld, *J. Chem. Phys.*, *20* (1952) 1591.
13 F. I. Tanczos, *J. Chem. Phys.*, *25* (1956) 439.
14 K. F. Herzfeld and T. A. Litovitz, *The Absorption and Dispersion of Ultrasonic Waves*, Academic Press, New York, 1959.
15 H. K. Shin, *J. Chem. Phys.*, *42* (1965) 59.
16 K. Kear and E. W. Abrahamson, *J. Photochem.*, *3* (1975) 409.
17 P. G. Dickens, J. W. Linnett and O. Sovers, *Discuss. Faraday Soc.*, *33* (1962) 52.

18 M. Braithwaite, J. A. Davidson and E. A. Ogryzlo, *J. Chem. Phys.*, *65* (1976) 771.
19 M. Braithwaite, E. A. Ogryzlo, J. A. Davidson and H. I. Schiff, *Chem. Phys. Lett.*, *42* (1976) 158.
20 G. Herzberg, *Molecular Spectra and Molecular Structure*, Vol. I, *Spectra of Diatomic Molecules*, Van Nostrand Reinhold, New York, 2nd edn., 1950.
21 J. D. Lambert, *Vibrational and Rotational Relaxation in Gases*, Clarendon, Oxford, 1977.
22 J. O. Hirschfelder, C. F. Curtiss and R. B. Bird, *Molecular Theory of Gases and Liquids*, Wiley, New York, 1954.
23 I. T. N. Jones and K. D. Bayes, *J. Chem. Phys.*, *57* (1972) 1003.
24 D. W. Oxtoby, *Adv. Chem. Phys.*, *47* (2) (1982) 487.
25 T. A. Litovitz, *J. Chem. Phys.*, *26* (1957) 469.
W. M. Madigosky and T. A. Litovitz, *J. Chem. Phys.*, *34* (1961) 489.
26 C. Delalande and G. M. Gale, *J. Chem. Phys.*, *71* (1979) 4804.
27 C. Delalande and G. M. Gale, *J. Chem. Phys.*, *73* (1980) 1918.
28 J. Chesnoy, *Chem. Phys.*, *83* (1984) 283.
29 B. Faltermeier, R. Protz, M. Maier and E. Werner, *Chem. Phys. Lett.*, *74* (1980) 425.
30 B. Faltermeier, R. Protz and M. Maier, *Chem. Phys.*, *62* (1981) 377.
31 T. Einwohner and B. J. Alder, *J. Chem. Phys.*, *49* (1968) 1458.
32 T. Boublik, *J. Chem. Phys.*, *53* (1970) 471.
33 G. A. Mansoori, N. F. Carnahan, K. E. Starling and T. W. Leland, Jr., *J. Chem. Phys.*, *54* (1971) 1523.

*Note added in proof*

Equation (6) of this paper is obtained by evaluating approximately the thermal average of the transition probability with the Laplace method [34]. The numerical evaluation of the integral is expected to give more accurate results at low temperatures. However, for the $^{16}O_2$–$^{18}O_2$ mixtures no significant differences were found between the results of eqn. (6) and the numerical integration.

34 H. K. Shin, *J. Chem. Phys.*, *55* (1971) 5233; *57* (1972) 1363.